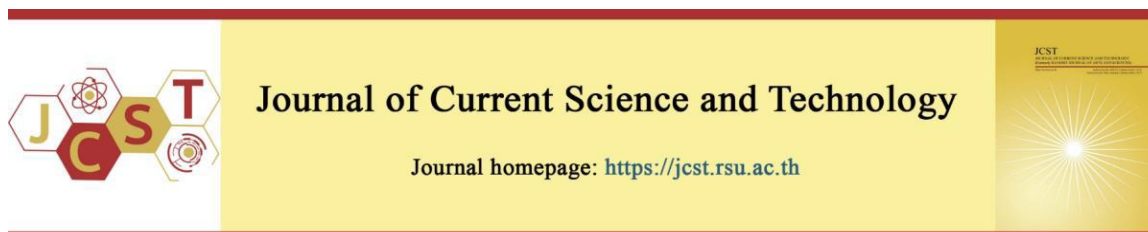


Cite this article: Phae-ngam, W., Prathumsit, J., Gitgeatpong, G., Chaikereee, T., Bodinthitukul, N., Lertvanithphol, T., Horprathum, M., & Jutarosaga, T. (2024). High-rate deposition of crystalline TiHfN ultra-thin films by closed-field dual-cathode DC unbalanced reactive magnetron sputtering without external substrate heating. *Journal of Current Science and Technology*, 14(3), Article 48. <https://doi.org/10.59796/jcst.V14N3.2024.48>



## High-rate Deposition of Crystalline TiHfN Ultra-thin Films by Closed-field Dual-cathode DC Unbalanced Reactive Magnetron Sputtering without External Substrate Heating

Wuttichai Phae-ngam<sup>1</sup>, Jedsada Prathumsit<sup>1,\*</sup>, Ganatee Gitgeatpong<sup>1</sup>, Tanapoj Chaikereee<sup>2</sup>, Nutdanai Bodinthitukul<sup>3</sup>, Tossaporn Lertvanithphol<sup>4</sup>, Mati Horprathum<sup>4</sup>, and Tula Jutarosaga<sup>3</sup>

<sup>1</sup>Faculty of Science and Technology, Phranakhon Rajabhat University, Bangkok, Bangkok 10220, Thailand

<sup>2</sup>Department of Electrical Technology Education, Faculty of Industrial Education and Technology, King Mongkut's University of Technology Thonburi, Bangkok 10140, Thailand

<sup>3</sup>Thin Film Technology Research Laboratory, Department of Physics, Faculty of Science, King Mongkut's University of Technology Thonburi, Bangkok 10140, Thailand

<sup>4</sup>Opto-Electrochemical Sensing Research Team, National Electronics and Computer Technology Center, Pathum Thani 12120, Thailand

\*Corresponding author; E-mail: [jedsada\\_19@hotmail.com](mailto:jedsada_19@hotmail.com)

Received 3 February 2024; Revised 12 March 2024; Accepted 21 March 2024  
Published online 1 September 2024

### Abstract

High deposition rate titanium hafnium nitride (TiHfN) ultra-thin film deposition was successfully prepared by closed-field dual-cathode DC unbalanced reactive magnetron sputtering. All prepared films were polycrystalline. The morphology and atomic composition of the TiHfN ultra-thin film were characterized by field-emission scanning electron microscopy (FE-SEM) and energy dispersive spectroscopy (EDS). The columnar structure could be promoted by increasing the deposition time. Lastly, the surface-enhanced Raman scattering (SERS) activity was investigated by Rhodamine 6G (R6G) drop-dried TiHfN ultra-thin film surface. The TiHfN ultra-thin films deposited at 20 s were found to have a high SERS activity, whose detection of R6G molecule at  $10^{-5}$  M. The result could open preliminary studies on ternary transition metal nitride (TTMN) thin films for the alternative plasmonic sensors as SERS chips.

**Keywords:** *TiHfN; sputtering; SERS; crystalline; unheated substrate*

### 1. Introduction

Over the past decade, coating transition metal nitride (TMN) thin films has attracted growing interest from research and engineering due to their significance in a wide industrial application for their high thermal stability and excellent mechanical and tribological properties (Maksakova et al., 2019; Chang et al., 2022; Mareus et al., 2020) The TMN thin films such as titanium nitride (TiN) and hafnium nitride (HfN) were also of interest as alternative plasmonic materials for reusable surface enhancement Raman scattering (SERS) substrate due to their high electron conductivity,

high melting point, and cost-effective material (Promjantuk et al., 2023; Beliaev et al., 2023; Krajczewski et al., 2023; Sucheewa et al., 2022). Moreover, the ternary transition metal nitride (TTMN) films, i.e., titanium zirconium nitride (TiZrN) and titanium hafnium nitride (TiHfN), have great significance to be explored as plasmonic materials because of their excellent structural stability and tunability in plasmonic properties (Ran et al., 2019; Javed et al., 2023). Among them, the TiHfN thin film gained interest because the TiN and HfN possessed high electron conductivity, high melting point, and excellent

SERS performance (Krajczewski et al., 2023; Sucheewa et al., 2022); however, ternary TiHfN was rarely reported.

Several deposition techniques have been used to prepare TTMN thin film, including cathodic arc deposition (Hasegawa, & Suzuki, 2004; Kaya, & Ulutan, 2022), pulsed laser deposition (Cai et al., 2014), and reactive magnetron sputtering performance (Phaengam et al., 2019; Chiu et al., 2020). Reactive magnetron sputtering was most common and famous for depositing TTMN thin films. It has high reproducibility, large surface area coating, easily adjustable deposition parameters, and the ability to control the film composition using a co-magnetron sputtering technique. However, two significant problems with preparing nitride films by reactive sputtering were the low deposition rate and difficulty promoting crystallinity. Our previous report discusses the closed-field dual-cathode DC unbalanced reactive magnetron sputtering, offering a high deposition rate and crystalline TMMN films without external heating or biasing during the film deposition (Chaiyakun et al., 2020), which could be a good candidate for the manufacturing process due to reduced production costs and high productivity.

## 2. Objectives

In this study, the TiHfN ultra-thin films have been deposited by the closed-field dual-cathode DC unbalanced reactive magnetron sputtering. The effect of deposition time on the crystal structure, morphology, and chemical composition has been investigated. The SERS activity of the prepared TiHfN ultra-thin films has also been preliminarily investigated.

## 3. Materials and methods

The TiHfN ultra-thin films were deposited onto silicon (100) wafer substrates by closed-field dual-cathode DC unbalanced reactive magnetron sputtering using 3-inch diameter Ti (99.95%) and Hf (99.95%). The silicon substrates were cleaned by ultrasonic in acetone, isopropanol, and DI water and blow-dried with N<sub>2</sub> before being loaded into the deposition chamber. The argon (Ar) and nitrogen (N) were used as sputtering and reactive gases and introduced into the deposition chamber with gas flow rates at 10 and 2.5 sccm (operated pressure at  $3 \times 10^{-3}$  mbar), respectively. Before TiHfN ultra-thin film deposition, the deposition chamber was pumped down to a base pressure of  $5 \times 10^{-5}$  mbar using a series of diffusion and mechanical rotary pumps. The sputtering currents of Ti and Hf targets were set at 250 mA and 1.5 A, respectively. The deposition times were varied from 5 to 20 sec. Further details on

the sputtering cathode part and closed-field dual-cathode DC unbalanced magnetron sputtering system design were reported in the previous publication (Chaiyakun et al., 2020).

**Table 1** Deposition condition of sputtered TiHfN ultra-thin films by closed-field dual-cathode DC unbalanced reactive magnetron sputtering

Deposition parameter	
Based pressure	$5 \times 10^{-5}$ mbar
Operated pressure	$3 \times 10^{-3}$ mbar
N <sub>2</sub> flow rate	2.5 sccm
Ar flow rate	10.0 sccm
Ti sputtering current	150 mA
Hf sputtering current	1.5 A
Deposition time	5-20 s

The morphology of TiHfN ultra-thin films was examined by field-emission scanning electron microscopy (FESEM; Hitachi, SU8030). The film crystallinity was characterized by grazing incidence X-ray diffraction (GIXRD; RigakuTtraz III). The compositions of the TiHfN ultra-thin films were investigated using energy dispersive spectroscopy (EDS). Lastly, the SERS measurement, 2.0  $\mu$ L droplets of the R6G aqueous solution with different concentrations were dropped onto the prepared samples and then dried at room temperature. The dried analyte solutions were analyzed with a Horiba LabRam HR Evolution with a 532 nm laser excitation at 0.44 mW. The objective lens and exposure time were 10X and 5 s, respectively.

## 4. Result and discussion

The cross-section and surface morphologies of the TiHfN ultra-thin films deposited at different deposition times are shown in Figure 1. The cross-section images were acquired to determine the average film thickness. Note that each thickness was measured at 10 positions on separated samples. From the results, the average thickness increases from  $17.8 \pm 1$  nm to  $46.4 \pm 1.1$  nm with increasing deposition time (Figure 1(a)-(d)). These results indicate that our preparation technique has a very high deposition rate of 1.81 nm/s, as shown in Figure 1(e). All TiHfN ultra-thin films exhibited dense with good adhesion to the Si substrate and a smooth surface without cracks. The columnar structure could be observed for the film deposited at 15 and 20 s, which could be related to the high kinetic energy of sputtered atoms due to the high magnetic field strength of the dual magnetron cathode.

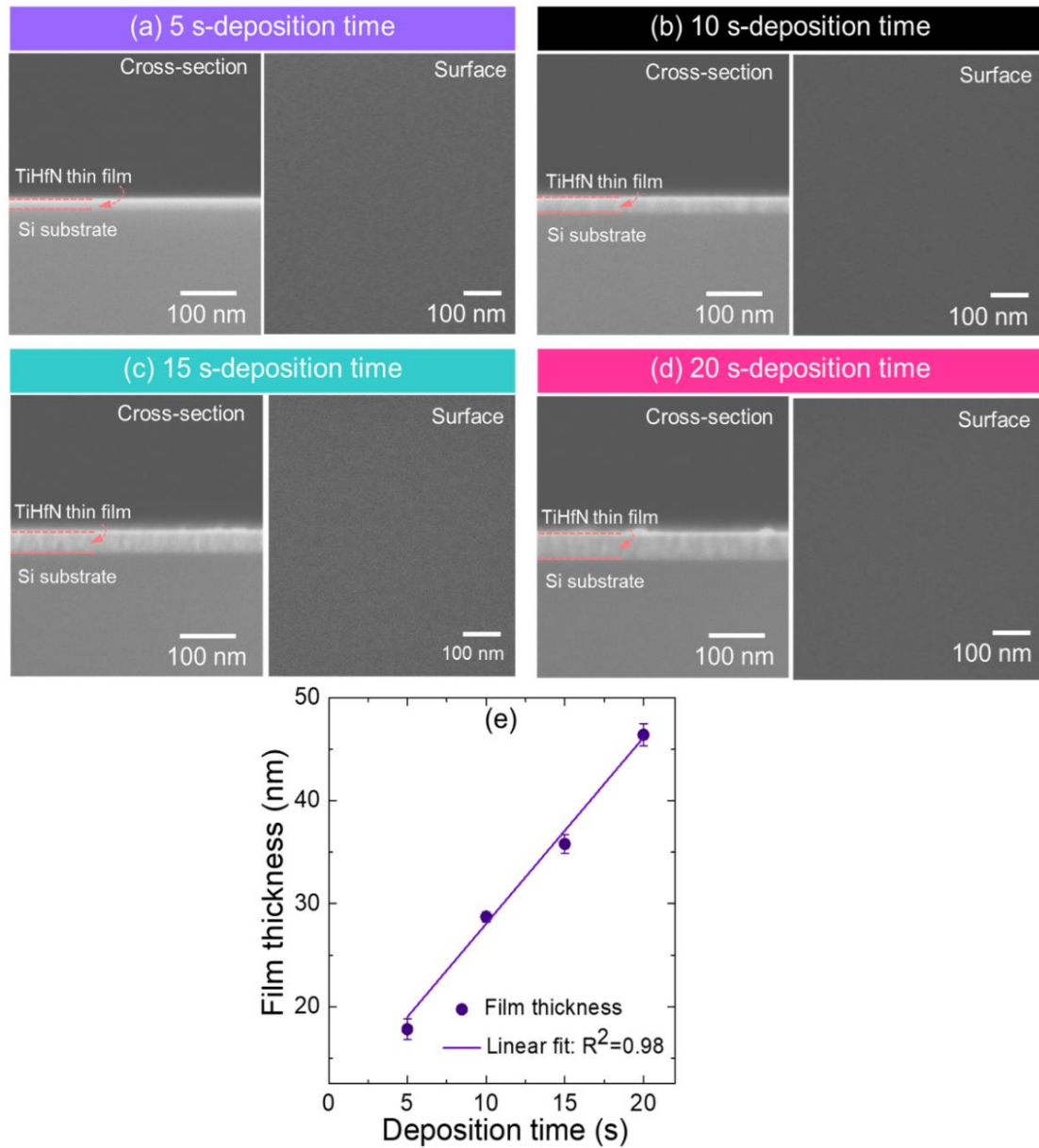


**Figure 1** (a)-(d) Cross-sectional and surface views of TiHfN ultra-thin films deposited at different times: (a) 5 s, (b) 10 s, (c) 15 s, and (d) 20 s. (e) Film thickness as a function of deposition time.

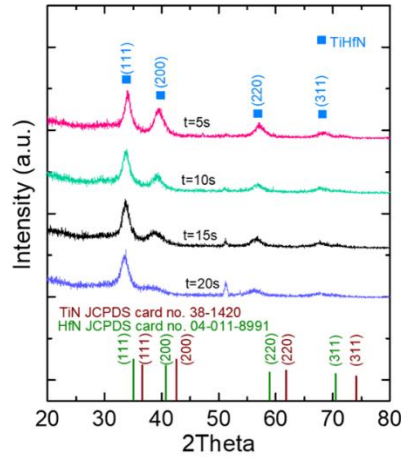


**Figure 2** GIXRD patterns of the TiHfN ultra-thin films prepared at different deposition times

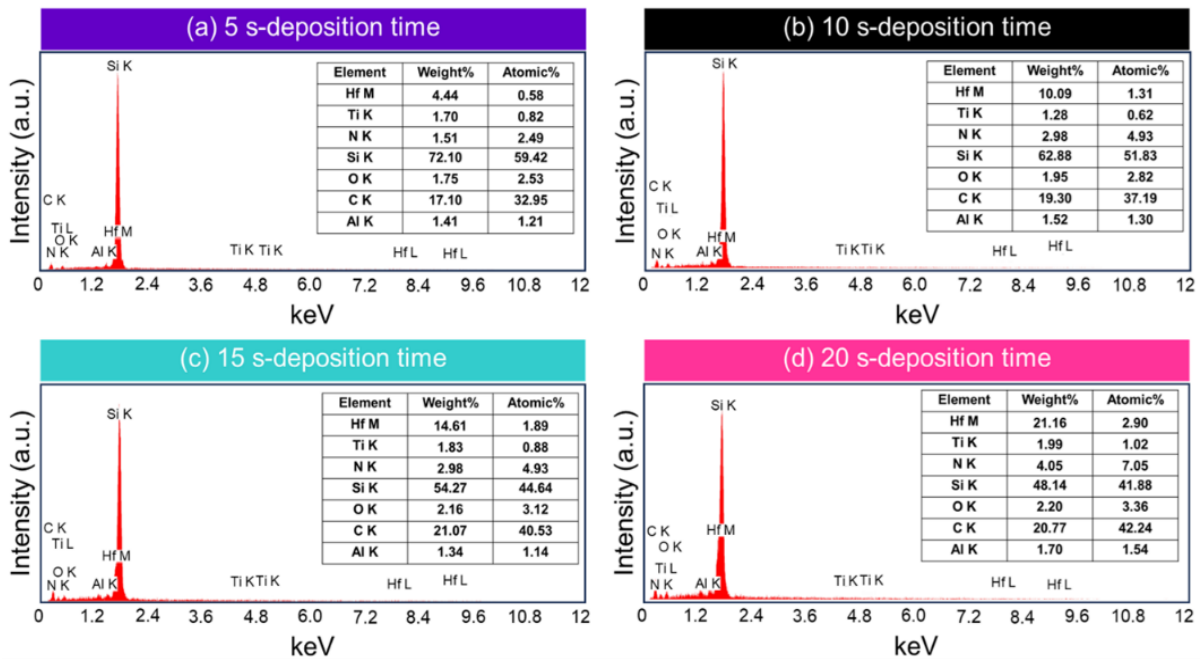


**Figure 3** Typical EDS spectra and atomic composition percentages of TiHfN ultra-thin films deposited at different times: (a) 5 s, (b) 10 s, (c) 15 s, and (d) 20 s.

Figure 2 shows the GIXRD pattern of the TiHfN ultra-thin films deposited at different deposition times. All prepared samples showed crystallinity with face-centered cubic (FCC) structures. Increasing deposition time was found to increase the film's crystalline content. This result indicated that the closed-field dual-cathode DC unbalanced reactive magnetron sputtering can promote film crystallinity without external heating during film deposition, with a high deposition rate. The GIXRD peaks of the (200) plane increased as the deposition time increased, which could result from

enhanced thermal energy from localized heating on the film surface (Taga, & Takahasi, 1997; Lee et al., 1996).

The chemical composition of the TiHfN ultra-thin films was analyzed using the EDS technique. Figure 3(a)-(d) shows the typical EDS spectrum of the TiHfN ultra-thin films deposited at different deposition times. The EDS spectrum shows characteristic Ti, Hf, and N peaks. This confirmed that our prepared films were composed of Ti, Hf, and N elements. However, O, C, and Al peaks were also detected as contamination and oxide layer formation

on the film surface. In addition, the prominent presence of Si element from the substrate was due to the beam size and penetration depth from EDS being in the micron scale. The inset table in Figure 3(a)-(d) shows the weight and atomic percentage analysis of all prepared samples. The results showed that small differences in the deposition time did not significantly impact the film's chemical composition.

To preliminarily investigate the SERS activity, 2  $\mu$ L of R6G solution at  $10^{-4}$  M was dropped onto the prepared TiHfN ultra-thin films. The average Raman spectra data was collected from ten different areas on each substrate. In Figure 4(a), the strong peaks at 614, 771, 1187, 1365, 1507, 1574, and 1651  $\text{cm}^{-1}$  assignments to C-C-C in-plane bending, C-H in-plane bending, C-H out-of-plane bending, C-C stretching, C-C stretching, C-C stretching and C-C stretching of R6G (Cheng et al., 2010; Zhang et al., 2023), respectively, were clearly seen from average SERS spectra of all prepared samples. Note that the small SERS spectra of  $10^{-4}$  M-R6G could be detected on the Si substrate. The result indicated that as the deposition time increases, the intensity of the Raman peak at 1365  $\text{cm}^{-1}$  increases, which might be due to the effect of the film morphology and crystalline nature of the film (Zhu et al., 2016; Wang et al., 2022). In addition, the TiHfN ultra-thin film deposited at 20 s exhibited

good SERS sensitivity with a detection limit at  $10^{-5}$  M, as shown in Figure 4(b).

## 5. Conclusion

In conclusion, the TiHfN ultra-thin films have been deposited by closed-field dual-cathode DC unbalanced reactive magnetron sputtering. The observed columnar structure within 20 s-deposition time can be explained by the high adatom energy deposition enabled by the dual magnetron cathode's high magnetic field strength. The result indicated that the crystallinity of the TiHfN ultra-thin film could be achieved without external substrate heating during the film deposition. The degree of film crystalline increases with increased deposition time. The SERS activity of the TiHfN ultra-thin films was successfully preliminarily studied with the R6G solution. It was found that the TiHfN ultra-thin films prepared at 20 s exhibit high crystallinity and high SERS intensity. The trace level down to  $10^{-5}$  M of the R6G was well detected. Our results indicate that the TiHfN ultra-thin films could be an alternative plasmonic sensing material for SERS platforms. Further study for optimizing the deposition conditions of TiHfN thin films as SERS substrates has been carried out, and the results will be published in the near future.

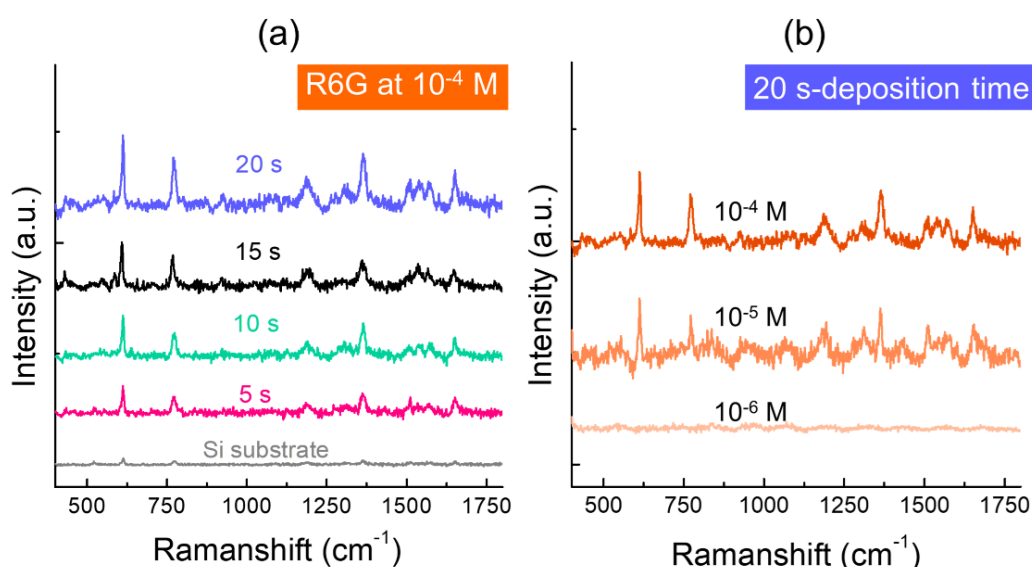


**Figure 4** (a) SERS spectra for  $10^{-4}$  M-R6G detection of the TiHfN ultra-thin films at different deposition times and (b) quantitative detection of the R6G at various concentrations on the TiHfN ultra-thin film deposited at 20 s.

## 6. Acknowledgements

This research work was supported by Phranakhon Rajabhat University and Thailand Science Research and Innovation.

## 7. References

- Beliaev, L. Yu., Shkondin, E., Lavrinenko, A. V., & Takayama, O. (2023). Optical properties of plasmonic titanium nitride thin films from ultraviolet to mid-infrared wavelengths deposited by pulsed-DC sputtering, thermal and plasma-enhanced atomic layer deposition. *Optical Materials*, 143, Article 114237. <https://doi.org/10.1016/j.optmat.2023.114237>.
- Cai, H., You, Q., Hu, Z., Guo, S., Yang, X., Sun, J., ... & Wu, J. (2014). Synthesis of high Al content Al<sub>x</sub>Ga<sub>1-x</sub>N ternary films by pulsed laser co-ablation of GaAs and Al targets assisted by nitrogen plasma. *Journal of Alloys and Compounds*, 616, 137-141. <https://doi.org/10.1016/j.jallcom.2014.07.090>
- Chaiyakun, T., Phae-ngam, W., & Prathumsit, J. (2020). High Deposition Rate of Dual-cathode DC Unbalanced Magnetron Sputtering. *American Journal of Applied Sciences*, 17(1), 231-239. <https://doi.org/10.3844/ajassp.2020.231.239>
- Chang, Y. Y., Chang, B. Y., & Chen, C. S. (2022). Effect of CrN addition on the mechanical and tribological performances of multilayered AlTiN/CrN/ZrN hard coatings. *Surface and Coatings Technology*, 433, Article 128107. <https://doi.org/10.1016/j.surfcoat.2022.128107>
- Cheng, C., Yan, B., Wong, S. M., Li, X., Zhou, W., Yu, T., ... & Fan, H. J. (2010). Fabrication and SERS performance of silver-nanoparticle-decorated Si/ZnO nanotrees in ordered arrays. *ACS Applied Materials & Interfaces*, 2(7), 1824-1828. <https://doi.org/10.1021/am100270b>
- Chiu, K. A., Fu, C. W., Fang, Y. S., Do, T. H., Shih, F. H., & Chang, L. (2020). Heteroepitaxial growth and microwave plasma annealing of DC reactive sputtering deposited TiZrN film on Si (100). *Surface and Coatings Technology*, 394, Article 125873. <https://doi.org/10.1016/j.surfcoat.2020.125873>
- Hasegawa, H., & Suzuki, T. (2004). Effects of second metal contents on microstructure and micro-hardness of ternary nitride films synthesized by cathodic arc method. *Surface and Coatings Technology*, 188, 234-240. <https://doi.org/10.1016/j.surfcoat.2004.08.033>
- Javed, M. U., Yang, J. W., Kumari, S., Mustaqeem, M., Peng, T. Y., Yang, L. C., ... & Kaun, C. C. (2023). Tailoring the plasmonic properties of complex transition metal nitrides: A theoretical and experimental approach. *Applied Surface Science*, 641, Article 158486. <https://doi.org/10.1016/j.apsusc.2023.158486>
- Kaya, E., & Ulutan, M. (2022). Tribomechanical and microstructural properties of cathodic arc-deposited ternary nitride coatings. *Ceramics International*, 48(15), 21305-21316. <https://doi.org/10.1016/j.ceramint.2022.04.097>
- Krajczewski, J., Michałowska, A., Čtvrtilík, R., Nožka, L., Tomáščík, J., Václavek, L., ... & Solarska, R. (2023). The battle for the future of SERS-TiN vs Au thin films with the same morphology. *Applied Surface Science*, 618, Article 156703. <https://doi.org/10.1016/j.apsusc.2023.156703>
- Lee, Y. E., Lee, J. B., Kim, Y. J., Yang, H. K., Park, J. C., & Kim, H. J. (1996). Microstructural evolution and preferred orientation change of radio-frequency-magnetron sputtered ZnO thin films. *Journal of Vacuum Science & Technology A: Vacuum, Surfaces, and Films*, 14(3), 1943-1948. <https://doi.org/10.1116/1.580365>
- Maksakova, O. V., Simočs, S., Pogrebniak, A. D., Bondar, O. V., Kravchenko, Y. O., Koltunowicz, T. N., & Shaimardanov, Z. K. (2019). Multilayered ZrN/CrN coatings with enhanced thermal and mechanical properties. *Journal of Alloys and Compounds*, 776, 679-690. <https://doi.org/10.1016/j.jallcom.2018.10.342>
- Mareus, R., Mastail, C., Anđay, F., Brunetière, N., & Abadias, G. (2020). Study of columnar growth, texture development and wettability of reactively sputter-deposited TiN, ZrN and HfN thin films at glancing angle incidence. *Surface and Coatings Technology*, 399, Article 126130. <https://doi.org/10.1016/j.surfcoat.2020.126130>
- Phae-ngam, W., Horprathum, M., Chananonawathorn, C., Lertvanithphol, T., Samransuksamer, B., Songsiriritthigul, P., Nakajima, H. & Chaiyakun, S. (2019). Oblique angle deposition of nanocolumnar TiZrN films via reactive magnetron co-sputtering technique: The influence of the Zr target

- powers, *Current Applied Physics*, 19(8), 894-901.  
<https://doi.org/10.1016/j.cap.2019.05.002>.
- Promjantuk, C., Lertvanithphol, T., Limsuwan, N., Limwichean, S., Wongdamnern, N., Sareein, T., ... & Klamchuen, A. (2023). Spectroscopic study on alternative plasmonic TiN-NRs film prepared by R-HiPIMS with GLAD technique, *Radiation Physics and Chemistry*, 202, Article 110589.  
<https://doi.org/10.1016/j.radphyschem.2022.110589>.
- Ran, Y., Lu, H., Zhao, S., Jia, L., Guo, Q., Gao, C., ... & Wang, Z. (2019). Structural and plasmonic properties of  $Ti_xZr_{1-x}Ny$  ternary nitride thin films. *Applied Surface Science*, 476, 560-568.  
<https://doi.org/10.1016/j.apsusc.2019.01.108>
- Sucheewa, N., Wongwiriyan, W., Klamchuen, A., Obata, M., Fujishige, M., Takeuchi, K., ... & Nukeaw, J. (2022). Tailoring properties of hafnium nitride thin film via reactive gas-timing RF magnetron sputtering for surface enhanced-raman scattering substrates. *Crystals*, 12(1), 78.  
<https://doi.org/10.3390/cryst12010078>
- Taga, Y., & Takahasi, R. (1997). Role of kinetic energy of sputtered particles in thin film formation. *Surface Science*, 386(1-3), 231-240. [https://doi.org/10.1016/S0039-6028\(97\)00313-0](https://doi.org/10.1016/S0039-6028(97)00313-0)
- Wang, X., Wu, Z., Wei, Y., Wu, M., Chen, Y., Hu, S., ... & Bu, J. (2022). Synthesis and SERS activity of niobium nitride thin films via reduction nitridation of sol-gel derived films. *Optical Materials*, 123, Article 111879.  
<https://doi.org/10.1016/j.optmat.2021.111879>
- Zhang, P., Jin, Y., & Fang, J. (2023). Triangular Au nanoparticle arrays based on flexible materials as temperature-sensitive SERS substrates, *Optical Materials*, 146, Article 114556.  
<https://doi.org/10.1016/j.optmat.2023.114556>
- Zhu, S., Xiao, L., & Cortie, M. B. (2016). Surface enhanced Raman spectroscopy on metal nitride thin films. *Vibrational Spectroscopy*, 85, 146-148.  
<https://doi.org/10.1016/j.vibspec.2016.03.019>